

Finite element modelling of self-supported transmission lines under tornado loading

A. Altalmas^{1a} and A.A. El Damatty^{*2}

¹AMEC plc, Alberta, Canada

²Department of Civil and Environmental Engineering, Western University, London, Ontario, Canada

(Received July 15, 2013, Revised December 2, 2013, Accepted December 3, 2013)

Abstract. Localized wind events, in the form of tornadoes and downbursts, are the main cause of the large number of failure incidents of electrical transmission line structures worldwide. In this study, a numerical model has been developed to study the behaviour of self-supported transmission lines under various tornado events. The tornado wind fields used were based on a full three-dimensional computational fluid dynamics analysis that was developed in an earlier study. A three-dimensional finite element model of an existing self-supported transmission line was developed. The tornado velocity wind fields were then used to predict the forces applied to the modelled transmission line system. A comprehensive parametric study was performed in order to assess the effects of the location of the tornado relative to the transmission line under F2 and F4 tornado wind fields. The study was used to identify critical tornado configurations which can be used when designing transmission line systems. The results were used to assess the sensitivity of the members' axial forces to changes in the location of the tornado relative to the transmission line. The results were then used to explain the behaviour of the transmission line when subjected to the identified critical tornado configurations.

Keywords: transmission tower; transmission line; tornado; wind; high intensity wind; finite element

1. Introduction

The disruption of electrical power due to the failure of a transmission line can cause overwhelming social, economic and financial losses to the affected area. Downbursts and tornadoes are localized wind storms that are sometimes referred to as High Intensity Wind (HIW) events, by the transmission-line industry. In addition to the negative social consequences, the direct costs of full restoration of an electric power system, once it has been damaged by a HIW event, can be very significant, as was the case after the 1996 event that occurred in Manitoba (McCarthy and Melsness 1996). A recent event took place on July 23rd, 2011 near Sarnia, Ontario where an F2 tornado damaged eight self-supported transmission towers belonging to Hydro One utility company. Hydro One estimated the cost associated with replacing the towers and restoring power to be \$5 million dollars.

*Corresponding author, Professor, E-mail: damatty@uwo.ca

^aM.E.Sc., E-mail: aaltalma@alumni.uwo.ca

Transmission line structures are typically designed for large scale wind events despite the fact that more than 80% of all weather-related failures are due to high intensity wind events (Dempsey and White 1996). The velocity profiles associated with localized HIW events are different than the boundary layer profile observed in large scale events. Also, tornadoes include a significant vertical velocity component in addition to the horizontal velocity component. These reasons have been the driving force behind the recent increase in efforts to develop a sustainable design process for transmission lines that incorporates the effects of HIW events.

A tornado is defined as a violently rotating column of air in contact with the ground and often visible as a funnel cloud (American Meteorological Society 2000). The localized nature of such events adds to the challenges associated with performing structural analysis of transmission line systems. The diameter of tornadoes rarely exceeds 1000m, which, depending on the location of the event relative to the transmission line, might lead to a significant unbalanced load to be applied to a section of the line (Fujita 1981). Another challenge arises from the fact that tornadoes are short-lived events and, therefore, reliable field measurements are difficult to obtain (Hangan and Kim 2008). Recent field measurements using Doppler radars were introduced by Sarkar, *et al.* (2005) and Lee and Wurman (2005) for two F4 tornadoes. Both laboratory and numerical simulations have been used to model tornadoes in order to overcome the limitations associated with obtaining full-scale data. A recent numerical simulation was performed by Hangan and Kim (2008) using the commercial program FLUENT (2005).

Few attempts have been made in the literature to investigate the structural behaviour of transmission line structures under the effect of tornado events. A study of the failure of a self-supported transmission tower under HIW was conducted by Savory *et al.* (2001). The tornado's wind field used did not include the vertical wind component associated with the tornado event. Another study conducted by Langlois (2007) focused on assessing the difference between various simplified tornado loading cases developed by American Society of Civil Engineers (ASCE) (1991, 2005), Behncke *et al.* (1994), Ishac and White (1995). The considered simplified loading conditions assumed constant wind pressures acting on the transmission tower, while neglecting the wind pressures on the conductors as well as the vertical component of the wind pressure associated with real tornadoes. Another study by Ahmad and Ansari (2009) examined the response of a self-supported transmission tower to tornado loading. The tornado model employed in the study was similar to the tornado model developed by Wen (1975). More recent studies were conducted by Hamada *et al.* (2010) and Hamada and El Damatty (2011), where a numerical model was developed to study the structural behaviour of guyed transmission lines under tornado loading. The tornado wind fields used were based on the numerical simulations conducted by Hangan and Kim (2008).

The current study focused on self-supported transmission lines. Numerical models were developed to investigate the structural behaviour of one electrical self-supported transmission line under tornado loading. The models involved simulations of an entire segment of the transmission line including the conductors and ground wires. The developed models were then used to conduct an extensive parametric study to assess the behaviour of self-supported transmission towers under tornadoes. The parametric study was conducted by varying the location of the tornado event relative to the transmission line. For each tornado location, a set of three-dimensional nonlinear finite element analysis was performed. The maximum tensile and compressive axial forces associated with the towers' members were reported. The results obtained were then used to identify critical tornado locations which can eventually be used in the development of equivalent critical tornado load cases.

2. Tornado Computational Fluid Dynamic (CFD) model

The tornado wind fields used in this study were based on a 3-D Computational Fluid Dynamics (CFD) simulation conducted by Hangan and Kim (2008) using the commercial program FLUENT (2005). The simulation was conducted at a steady-state with no time variation. The velocity field profile is a function of the cylindrical coordinate system (r, θ, z) . In addition, the velocity field data was averaged along the circumference, eliminating the variation of the velocity with θ and resulting in an axi-symmetric velocity field as a function of (r, z) . The tornado wind field used by Hangan and Kim (2008) to calibrate their numerical results was based on the full scale data provided by Sarkar *et al.* (2005). The CFD parameters were varied by Hangan and Kim (2008) in order to obtain a good match between the numerical results and the field measurements available.

The results indicated that the numerical data with a swirl ratio $S = 2$ provided a good simulation for the F4 tornado. Moreover, it was found that the CFD data had to be magnified using the following scales: velocity scale ratio $V_s = 13$; and length scale ratio $L_s = 4000$. These factors allowed for the maximum velocity of the CFD model to match the maximum velocity defined by the Fujita scale for an F4 tornado. The value of the tangential component was significantly larger than the values of the other two components and the peak velocity components for the tornado wind field occurred at three different height levels relative to the ground.

In the study conducted by Hamada *et al.* (2010), it was shown that the numerical data with a swirl ratio $S = 1$ provided a good simulation for the F2 tornado. The CFD data had to be magnified using the same magnification scales used for the F4 wind field. The magnification scales used were: velocity scale ratio $V_s = 13$; and length scale ratio $L_s = 4000$. The maximum tangential velocity for the F2 tornado was estimated to be 86 m/sec. More details on the employed scaling procedure can be found in Hamada *et al.* (2010).

3. Description of the transmission line system

The tower selected for the study had an overall height of 47.5 m as shown in Fig. 1. The cross-arms were located at a height of 35.1 m and had a width of 13.4 m. Conductors were connected to the tower at three locations. Each of the outer left and outer right conductors was attached to a single insulator 4.9 m long at a height of 30.3 m, which was allowed to swing in two perpendicular planes. The middle conductor was attached to the towers using two insulators each 5.9 m long at a height of 40 m. This tower type supported nine conductors that spanned between every two consecutive towers with a horizontal span of 420 m. The nine conductors were divided into three groups each consisting of three conductors in the form of an inverted triangle. Two ground wires were attached to the top of the towers for protection against lightning.

The transmission line was modelled using the finite element program SAP2000 (Computer and Structures Inc. 2008). The model consisted of five identical transmission towers spanning six bays. The middle tower was considered the tower of interest. This configuration was recommended by Shehata *et al.* (2005) in order to accurately transfer the cable forces to the tower of interest. The global coordinate system of the models was defined as follows: the X-axis was in the direction perpendicular to the transmission line, the Y-axis was in the direction parallel to the transmission line and the Z-axis was the vertical direction with the origin located at the centre of the tower of interest.

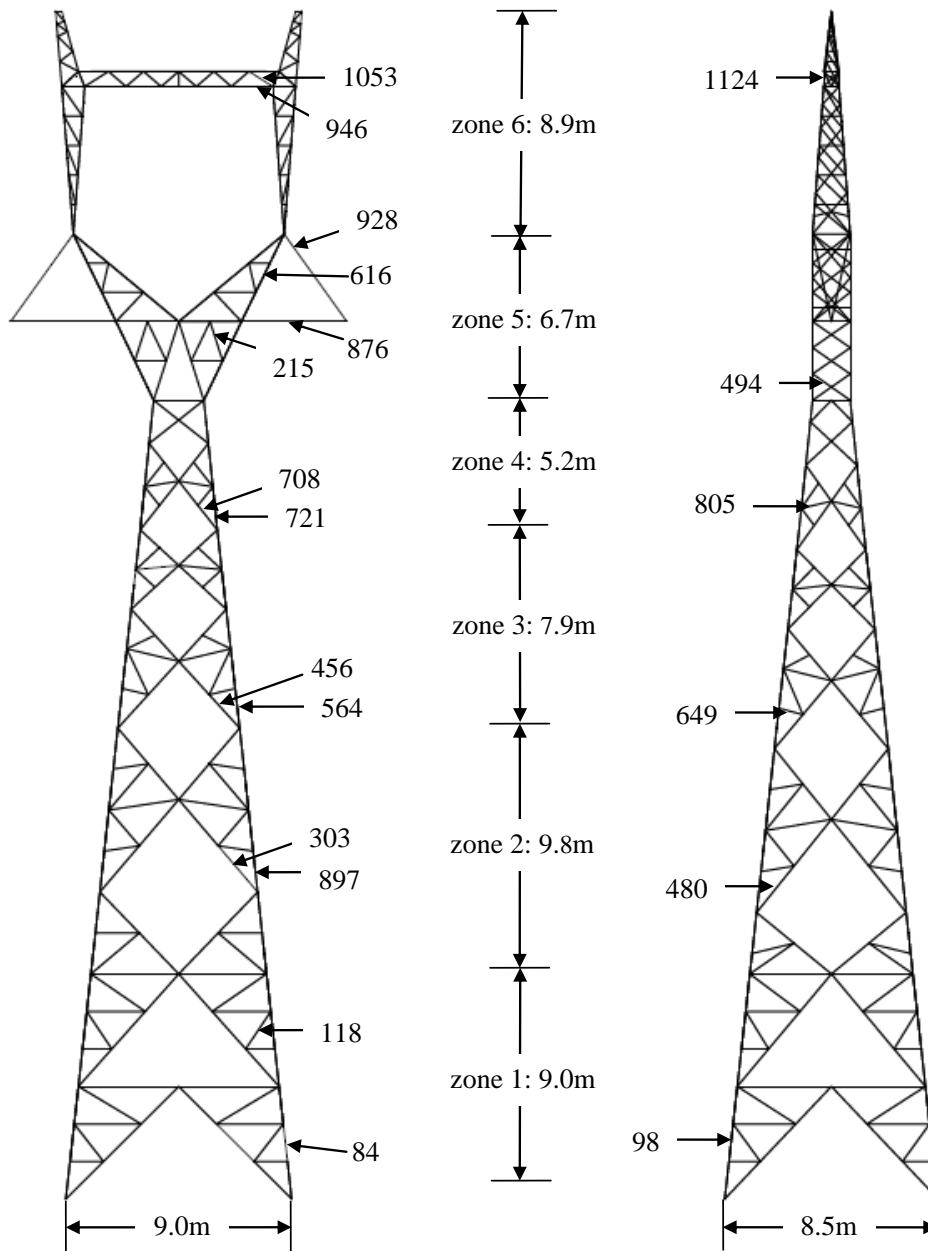


Fig. 1 Geometry of the modelled tower

Each tower member was modelled using a single three dimensional nonlinear frame element taking its own weight into account. Each element had two nodes with six degrees of freedom per node. The tower members were assumed to be rigidly connected which mimicked the behaviour of the multi-bolted connections used between the various members in the real tower.

A three-dimensional nonlinear cable element was used to model the conductors and the ground wires. Each cable was divided into thirty cable elements. Each cable element had two nodes with three translational degrees of freedom per node. The cable element simulated the nonlinear behaviour of the slender cables under the combined effects of self-weight, pretension forces and tornado wind loading. Geometric nonlinearities were considered in the model by including the P-delta effect in the analysis. The cables' stiffness matrix was calculated by taking into account the tension stiffening of the cables resulting from the target pretension forces. The tension stiffening was obtained by iterating the target load case nonlinearly until the pretension force of each cable was achieved.

Each insulator string was modelled using a single three dimensional truss element. Each element had two nodes with six degrees of freedom per node. Two internal hinges were assumed between the insulators and the tower cross-arms and between the insulators and the conductors. This mimicked the behaviour of the real tower by allowing the insulator strings and the conductors to rotate independent of each other. The tower was divided into six zones. Zones 1 to 4 and 6 were located in the main body of the tower, while zone 5 was the cross-arms' zone. Fig. 1 shows the geometry as well as the zones of the modelled tower. The figure also shows the twenty members selected to display the results of the study.

4. Evaluation of forces on the transmission line

The steps followed to evaluate the wind forces of the transmission line due to a tornado configuration are discussed below. This procedure has been automated through the development of a code using the programming language FORTRAN (Lahey Computer Systems Inc. 1999).

The wind force acting on any nodal point on the tower in the direction "i" was calculated using the equation provided in the ASCE No. 74 guidelines (2010).

$$F_i = \gamma_w Q K_z K_{zt} (V_i)^2 G C_{fi} A_i \quad (1)$$

Where "i" is the desired direction; F_i is the wind force in "i" direction (N); γ_w is a load factor; Q is a numerical constant; K_z is the velocity pressure exposure coefficient; K_{zt} is a topographic factor; V_i is the tornado velocity component in direction "i" (m/sec); G is the gust response factor; C_{fi} is the drag force coefficient in direction "i"; and A_i is the projected area of all the elements connected to the considered node and perpendicular to the direction "i"; $i=1$ and 2 represents the x and y directions, respectively.

The value of Q was taken to equal $0.5\rho_a$ where ρ_a is equal to 1.226 kg/m^3 . The values of G and K_z are equal to unity for tornado forces as recommended by the ASCE No. 74 guidelines (2010). No topographic variation was assumed in the study and therefore the value of K_{zt} was taken to equal unity. The values of C_{fi} for the tower were based on the solidity ratio approach as described in the ASCE No.74 Guidelines (2010). The factor C_{fi} for the conductors and the ground wires was assigned a constant value of 1 as recommended by the ASCE No. 74 Guidelines (2010). The projected area served by each node, A_i , was calculated. Finally, the force, F_i was calculated for all nodes at each height using the equation above. The forces were then distributed between the

windward and the leeward faces of the tower using the shielding factors recommended by NRCC (1990). More details about this procedure can be found in Shehata *et al.* (2005).

5. CIGRE simplified tornado loading

A comparison was made in this study with the internal forces obtained using the simplified F2 tornado loading recommended by the International Council on Large Electric Systems (CIGRE) (2009). This simplified tornado loading is similar to the provisions recommended by various codes and guidelines for the design for HIW events (ASCE 2010). The following two load cases are recommended by the CIGRE in order to simulate F2 tornadoes:

1. Uniform horizontal velocity applied on the tower only from any direction. CIGRE recommends neglecting the tornado effect on the conductors due to the tornado's relatively narrow width and the complexity of the force mechanism applied on the conductors. The self-weight of the members and the conductors was included.
2. Failure containment: transmission towers to be designed to withstand the extra longitudinal loads resulting from damaged conductors in a tornado event. In this load case, the tower was subjected to 25% of the force described in step 1. In addition to this load, the tower was subjected to longitudinal force equal to 70% of the every-day pretension force of the damaged conductor. For this load case, it was assumed that the worst case of either any two phases, or any phase and any ground wire can become damaged. This transmission line supported three phases, with each phase consisting of three bundled conductors.

For both load cases, and according to CIGRE (2009), the wind velocity was assumed to be equal to 60 m/sec. Eq. (1) was applied for both load cases in order to calculate the corresponding tower's nodal forces.

The values of the factors described above, except for the value of V_i , were used to allow comparison of the results. More details on simplified F2 tornado loading case of CIGRE can be found in Overhead Line Design Guidelines for Mitigation of Severe Wind Storm Damage (2009).

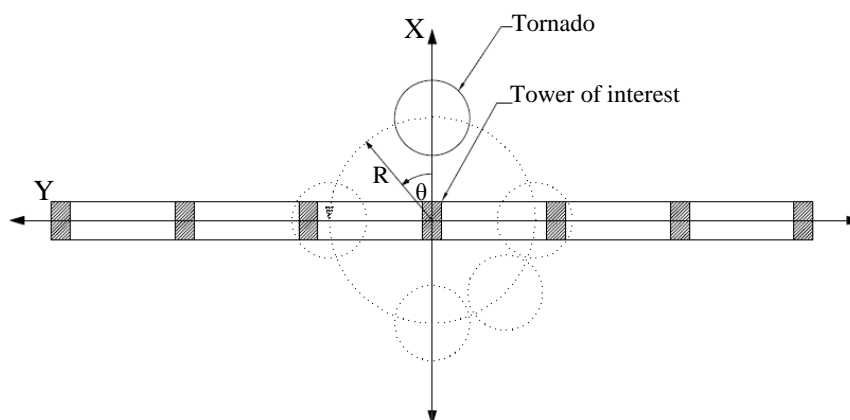


Fig. 2 Schematic diagram of the conducted parametric study

6. Case study

The parametric study was conducted by varying the location of the tornado relative to the tower. A nonlinear finite element analysis was carried out on the transmission line for each tornado location. The tornado's location relative to the tower of interest was defined by the polar coordinates R and θ , as shown in Fig. 2. The analyses were conducted in a quasi-static state despite the dynamic variation of the convective velocity of the tornadoes. This was justifiable since the used tornado velocity fields were calibrated with field measurements, which included two types of velocities. The first velocity type consisted of the tornado's internal wind velocities while the second velocity type consisted of the tornado's translational velocity. Also, previous studies including Darwish *et al.* (2010), Hamada *et al.* (2010), and Matheson and Holmes (1981), have shown that the dynamic effects of wind loading on transmission lines are not significant. This is due to the difference between the natural period of transmission lines and the natural period of the tornado loading as well as the relatively high aerodynamic damping of the cables.

The parametric study consisted of two parts. The first part included 121 cases for each tornado wind field. It was conducted using the three-dimensional F2 and F4 tornado wind fields as well as the two-dimensional F4 tornado wind field. In each case, the location of the tornado was determined by the parameters R and θ . The parameter R was varied from 0 m to 500 m with a step of 50 m. The parameter θ was varied from 0° to 330° with a step of 30° . The maximum and the minimum axial forces were then obtained for all tower members. The members' forces obtained from the analyses were then compared to the members' capacities, the maximum internal forces due to normal boundary layer wind, and the internal forces due to the equivalent two-dimensional tornado loading suggested in the CIGRE loading document (2009).

7. Results of the analysis

The results of the nonlinear parametric study are presented for the twenty selected members shown in Fig. 1. The members were classified according to their types: chord, or diagonal members. The diagonal (1) and diagonal (2) members were located in one of two planes: a plane perpendicular to the transmission line, referred to as diagonal (1); a plane parallel to the transmission line, referred to as diagonal (2). Three members, consisting of a chord and two diagonal members were selected for each zone. Two additional chord members were selected for the conductor cross arm area in zone 5. The peak internal forces, as well as the tornado locations associated with those peak forces, are listed below for each of the selected members. The tables also include the members' tensile and compressive capacities. The capacities of the members were calculated based on the procedure described in ASCE Standard 10-97 (2000).

7.1 Transmission tower under F4 tornado wind fields

The results of the parametric study conducted under the axisymmetric two-dimensional and the three-dimensional F4 tornado wind fields are listed in Table 1. The table also includes the members' tensile and compressive capacities for comparison with the results of the study. The tornado wind field had a maximum tangential velocity of 142 m/sec which occurred at a radius $r = 158$ m and a height $z = 28$ m. The maximum radial velocity component was 79 m/sec which acted

inward and occurred at a radius $r = 273$ m and at a height $z = 7$ m. The maximum axial velocity component was 62 m/sec which occurred at a radius $r = 246$ m and at a height $z = 158$ m.

The following observations were drawn from the results shown in the table below:

- The members' axial forces were sensitive to the location of the tornado relative to the tower.
- The majority of the tornado locations that led to the critical forces were the same under both the 3-D and the 2-D axi-symmetric F4 wind fields. The majority of the members had the same value for the parameter θ under both wind fields, while the value for the parameter R might vary by 50 metres from one wind field to the other.
- The difference between the axial forces resulting from the axi-symmetric and the 3-D data was relatively small. The percent difference between both sets of compression results was less than 10% for chord members.
- For the tensile load results, the percent difference between the axi-symmetric and the 3-D results was less than 5% for all chord members except for the lower chord member, which varied by 19%.
- The difference between the axial forces resulting from the axi-symmetric and the 3-D data was more pronounced for some of the diagonal members. The percent difference between both sets of results was as high as 100% for one diagonal member.
- The use of the simplified 2-D wind field gave reasonable results despite the fact that it did not allow for the wind instability in the lower region of the tornado system to be taken into account. This wind instability could only be simulated in the full 3-D analysis (Hangan and Kim 2008).
- For the chord members in zones 1 to 5, the critical tornado configuration leading to maximum compression force had an R value ranging between 300 m and 350 m, and θ value of 300° . The location of the tornado relative to the tower is shown in Fig. 3, labelled tornado location 1. For the same member, the critical tornado leading to maximum tensile force had an R value ranging between 300 m and 350 m, and θ value of 120° . The tornado in this case is also shown in Fig. 3, labelled tornado location 2.

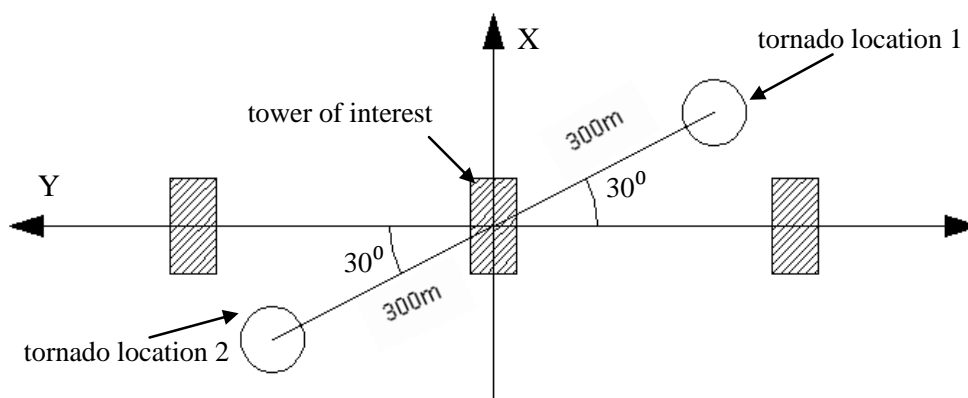


Fig. 3 Schematic diagram of the critical F4 tornado locations for chord members in zones 1 to 5

Table 1 Results under F4 tornado wind fields for the selected members (peak forces)

Zone	Member		Member Capacity (ASCE 10-97) Force (kN)	F4 tornado - 2D CFD			F4 tornado - 3D CFD		
	#	Type		Case			Case		
#	#	Type	Force (kN)	R (m)	θ (deg)	Force (kN)	R (m)	θ (deg)	Force (kN)
1	84	Chord	-716	300	300	-1984	300	300	-2020
			805	300	120	1865	300	120	1898
	118	Diagonal (1)	-58	150	330	-6	150	330	-7
			100	300	120	27	300	120	27
	98	Diagonal (2)	-56	150	330	-3	100	330	-1
			100	300	120	20	300	120	20
2	897	Chord	-624	350	300	-1729	300	300	-1765
			728	300	120	1594	300	120	1620
	303	Diagonal (1)	-155	150	270	-106	150	270	-113
			264	200	120	123	200	120	122
	480	Diagonal (2)	-125	200	330	-84	200	330	-88
			248	350	120	86	350	120	90
3	564	Chord	-494	350	300	-1617	300	300	-1656
			650	350	120	1459	300	120	1472
	456	Diagonal (1)	-146	350	270	-108	300	270	-121
			209	250	120	102	250	120	101
	649	Diagonal (2)	-51	300	120	-38	300	120	-38
			60	200	330	12	200	330	11
4	721	Chord	-493	350	300	-1360	350	300	-1412
			650	350	120	1294	400	120	1327
	708	Diagonal (1)	-154	350	270	-184	300	270	-190
			250	300	150	126	300	150	125
	805	Diagonal (2)	-58	350	120	-26	350	120	-27
			79	200	300	10	200	300	10
5	616	Chord	-376	300	300	-293	350	300	-316
			426	400	90	541	350	90	564
	928	Cross-arm's upper chord	-26	450	90	-143	450	90	-150
			162	250	150	125	200	150	128
	876	Cross-arm's lower chord	-340	400	90	-131	350	90	-137
			538	300	330	64	200	330	53
215	Diagonal (1)	-38	400	270	-5	400	270	-6	
		79	300	120	8	300	120	8	
494	Diagonal (2)	-108	250	0	-46	250	0	-47	
		162	500	270	34	450	270	39	
6	946	Chord	-189	250	270	-444	300	300	-442
			236	300	120	452	250	90	458
	1053	Diagonal (1)	-92	250	270	-208	300	270	-211
			134	250	120	178	250	120	179
	1124	Diagonal (2)	-80	350	270	-96	300	270	-99
			106	250	120	73	250	120	72

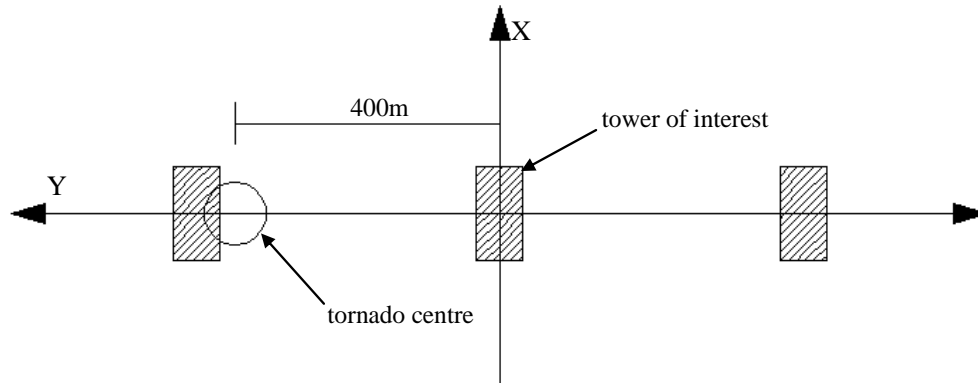


Fig. 4 Schematic diagram of the critical F4 tornado location for cross-arm's upper chord member in zone 5

- For the upper chord member in zone 5 (cross-arm zone), the maximum compressive force occurred where $R=400$ m and $\theta=90^{\circ}$. The location of the tornado relative to the tower is shown in Fig. 4.

- For a given member, the critical tornado location associated with the peak tensile load had the same R value as the critical tornado location associated with the peak compressive load.

- For a given member, the critical tornado location associated with the peak tensile load had a θ value that was 180° away from the critical tornado location associated with the peak compressive load.

- No general trend with regards to the critical tornado configuration associated with the diagonal members could be identified, as various members had different critical R and θ values.

- The axial forces resulting from F4 tornado wind field exceeded the compression capacity of 9 out of the 20 members selected, of which 6 were chord members. In these members, the axial forces due to F4 tornado loading ranged between one and three times the members' compression capacity with the exception of the upper chord member which exceeded its compression capacity by a factor of five.

- The axial forces resulting from F4 tornado wind field exceeded the tensile capacity of 7 out of the 20 members selected, of which 6 were chord members.

7.2 Transmission tower under F2 tornado wind field

The results of the parametric study conducted under the three-dimensional F2 tornado wind field are listed in Table 2. The peak axial tensile and compressive loads due to the tornado load for the selected chord, diagonal (1) and diagonal (2) members are provided in the table. The F2 tornado wind field had a maximum tangential velocity of 78 m/sec, which occurred at a radius $r = 96$ m and a height $z = 28$ m. The maximum radial velocity component was 49 m/sec, which acted inward and occurred at a radius $r = 146$ m and at a height $z = 6$ m. The maximum axial velocity component was 37 m/sec which occurred at a radius $r = 171$ m and at a height $z = 127$ m.

The table below also include the members' nominal tensile and compressive capacities as well as the axial forces due to the conventional boundary layer wind for comparison. The boundary

layer forces listed are the internal forces considered in designing the tower. They were calculated based on the Canadian Standards Association specification, CSA-C22.3 No. 1 (1976), assuming a reference wind velocity of 32.2 m/sec. The loads on the conductors and the ground wires due to their own weight as well as due wind were applied to the tower as concentrated point loads. The tables below also include the axial forces due to the simplified F2 tornado loading suggested by CIGRE (2009).

The following observations were drawn from the results shown in the table below:

- The influence of the F2 tornado locations relative to the tower on the axial forces was significant.
- The majority of the F2 tornado locations that lead to the critical cases had the same parameter θ as those under F4 tornado. This conclusion could not be extended to include the parameter R. This was expected since the vertical distribution of the velocity profiles was similar for both F2 and F4 wind fields but at different radial radius r .
- The axial forces due to F2 tornado were significantly less than those due to F4 tornado.
- For the chord members in zones 1 to 6, the maximum compression forces occurred at $\theta=300^\circ$. This is similar to the F4 tornado cases. However, no fixed value for the critical R-value was shown for the F2 tornado, as it varied between 100 m and 250 m. For the same members, the maximum tensile force occurred at $\theta=120^\circ$, also with different value of R.
- For a given member, the critical tornado location associated with the peak tensile load had the same R value as the critical tornado location associated with the peak compressive load.
- For a given member, the critical tornado location associated with the peak tensile load had a θ value that is 180° away from the critical tornado location associated with the peak compressive load.
- The axial compressive forces due to normal wind exceeded those due to F2 tornado in 9 of the considered members, two of which were chord members.
- The axial tensile forces due to normal wind exceeded those due to F2 tornado in 9 of the considered members, three of which were chord members.
- The simplified tornado loading by CIGRE underestimated the axial compressive forces in the selected chord members located in zones 1 to 3, and 6 when compared to the compressive forces resulting from F2 tornado loading. However, the axial forces in zones 4 and 5 due to CIGRE loading were higher than those due to F2 tornado loading. The discrepancy in the axial forces both tornado models could be attributed to the failure containment loading considered in the loading suggested in the CIGRE document.
- The simplified tornado loading by CIGRE underestimated the axial tensile forces in the selected chord members located in zones 1 to 3, and 6 when compared to the tensile forces resulting from F2 tornado loading. On the other hand, the CIGRE tornado loading overestimated the tensile forces in the chord members located in zones 4 and 5. This could also be attributed to the failure containment load case suggested by CIGRE.
- The cross-arm's upper chord member was subjected to large compressive axial force under the simplified tornado loading by CIGRE, unlike the case with F2 tornado wind field. This could also be attributed to the failure containment load case suggested by CIGRE, in order to account for the tornado's unbalanced loading. On the other hand, this unbalanced loading was inherently considered in the three-dimensional tornado wind field used.

Table 2 Results under F2 tornado wind field for the selected members (peak forces)

Zone #	Member		Member Capacity (ASCE 10-97) Force (kN)	Boundary Layer Force (kN)	CIGRE loading Force (kN)	F2 tornado - 3D CFD Case		
	#	Type				R (m)	θ (deg)	Force (kN)
1	84	Chord	-716	-388	-470	150	300	-588
			805	296	385	200	120	492
	118	Diagonal (1)	-58	-3	-4	250	300	-3
			100	3	4	250	120	5
	98	Diagonal (2)	-56	-1	-2	100	300	0
			100	1	2	200	120	3
2	897	Chord	-624	-376	-438	250	300	-520
			728	299	414	200	120	416
	303	Diagonal (1)	-155	-58	-58	150	300	-30
			264	56	56	100	120	32
	480	Diagonal (2)	-125	-39	-43	150	330	-28
			248	38	41	200	150	20
3	564	Chord	-494	-370	-426	250	300	-474
			650	299	437	300	120	371
	456	Diagonal (1)	-146	-59	-67	100	270	-27
			209	62	74	150	120	27
	649	Diagonal (2)	-51	-4	-5	200	120	-8
			60	5	6	250	300	6
4	721	Chord	-493	-383	-465	300	300	-404
			650	319	511	300	120	328
	708	Diagonal (1)	-154	-97	-113	250	300	-31
			250	104	124	200	120	30
	805	Diagonal (2)	-58	-2	-2	200	120	-5
			79	3	3	200	300	4
5	616	Chord	-376	-241	-264	350	270	-190
			426	95	162	350	90	90
	928	Cross-arm's upper chord	-26	-20	-82	400	90	-26
			162	76	91	450	270	51
	876	Cross-arm's lower chord	-340	-186	-196	350	90	-49
			538	171	195	350	270	15
	215	Diagonal (1)	-38	-2	-2	350	270	-1
			79	3	2	250	120	2
	494	Diagonal (2)	-108	-76	-101	450	90	-14
			162	72	102	450	270	10
6	946	Chord	-189	-38	-25	200	300	-115
			236	62	37	200	120	126
	1053	Diagonal (1)	-92	-24	-12	200	300	-50
			134	25	12	200	120	50
	1124	Diagonal (2)	-80	-7	-12	300	300	-19
			106	19	14	200	120	25

7.3 Sensitivity of the internal forces in the tower members to changing tornado configurations

The sensitivity of the axial forces in members to changes in the location of the centre of the tornado, relative to the centre of the tower of interest, was studied. The study was conducted using the axi-symmetric F4 tornado wind field. The location of the centre of the tornado relative to the tower was defined by the polar coordinates R and θ . The sensitivity study was performed using the same parametric study outlined above. Three chord members were selected for this study. The first member (#84) was located in the tower's main body while the other two members (#928, #876) formed the cross-arm's upper and lower chord members, respectively. The locations of the members can be seen in Fig. 1. The results of the study are shown in Fig. 5 to Fig. 10. The graphs were used to study the sensitivity of the members' internal forces; first, solely due to the variation of θ , and second, solely due to the variation of R . The variations of the internal forces were graphed for various θ values at two R values. The first R value was that associated with the critical case as listed in Table 1. The second R value was taken to equal 50 m. An R value of 50 m was selected because it was located near the lower end of the range. This allowed for a good comparison of the internal forces with respect to the two R values. Also, the variation of the internal force of each member was graphed for various R values and for the θ value associated with the critical case as listed in Table 1.

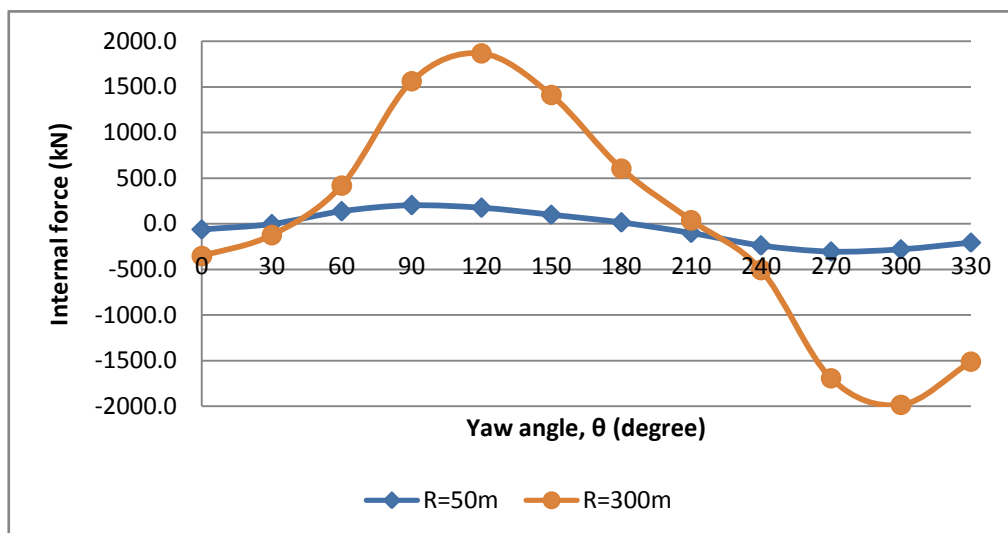


Fig. 5 Variation of the internal force in chord member #84 for various values of θ

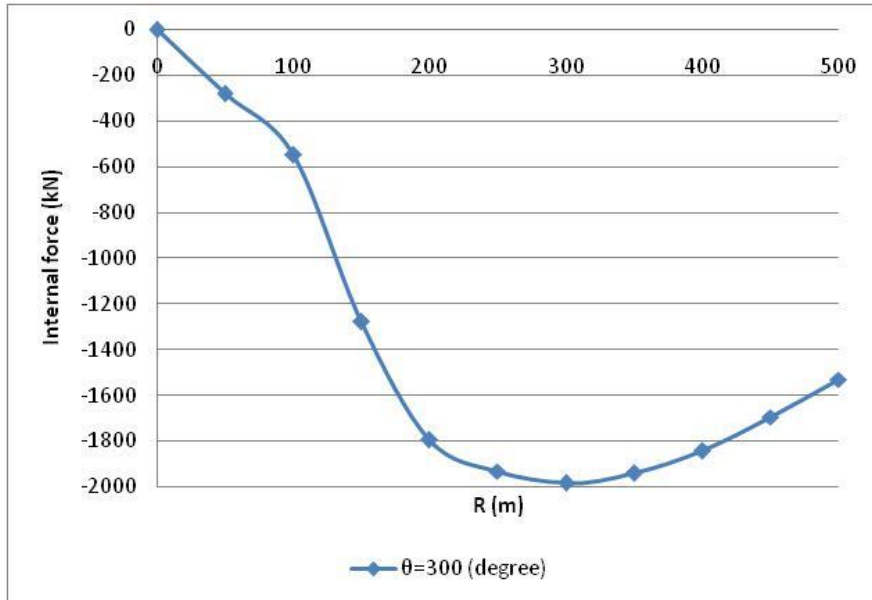


Fig. 6 Variation of the internal force in chord member #84 for various values of R

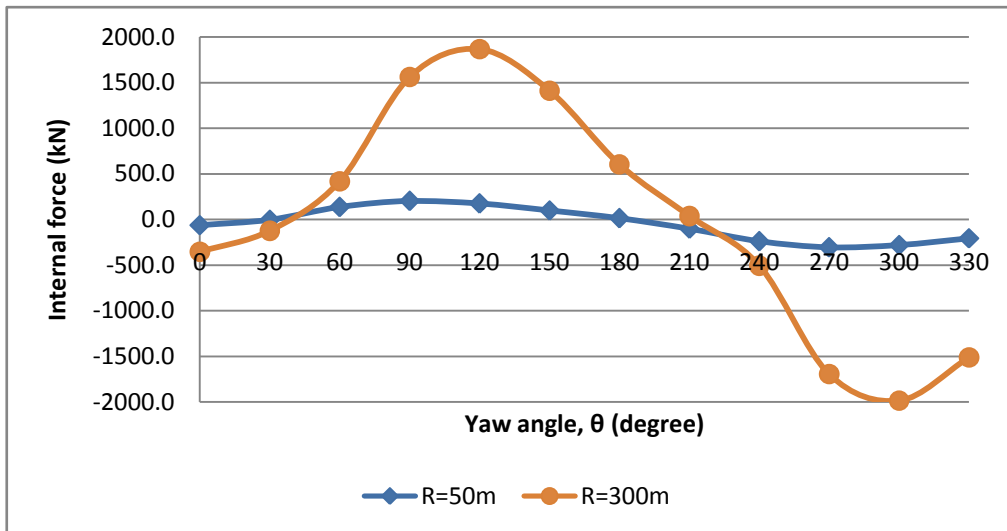


Fig. 7 Variation of the internal force in upper chord member #928 for various values of θ

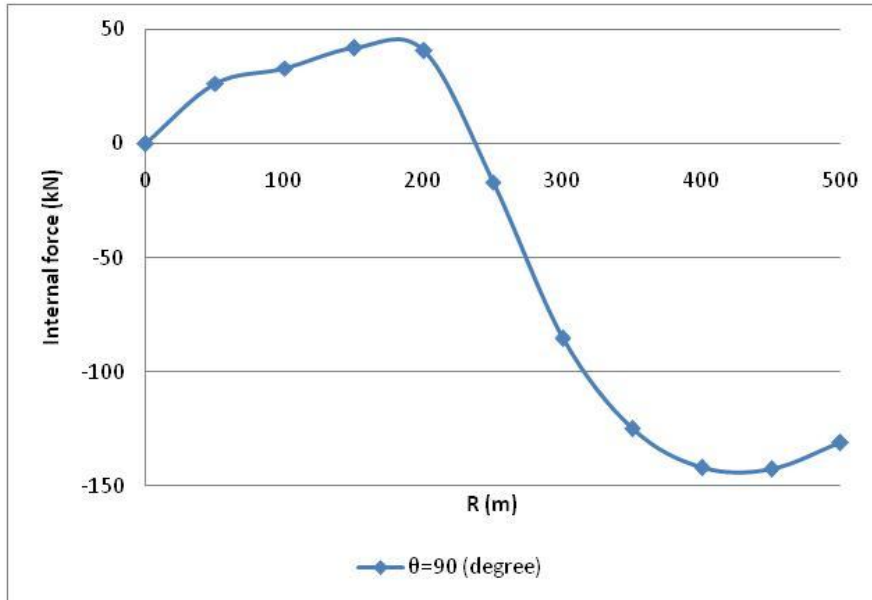


Fig. 8 Variation of the internal force in upper chord member #928 for various values of R

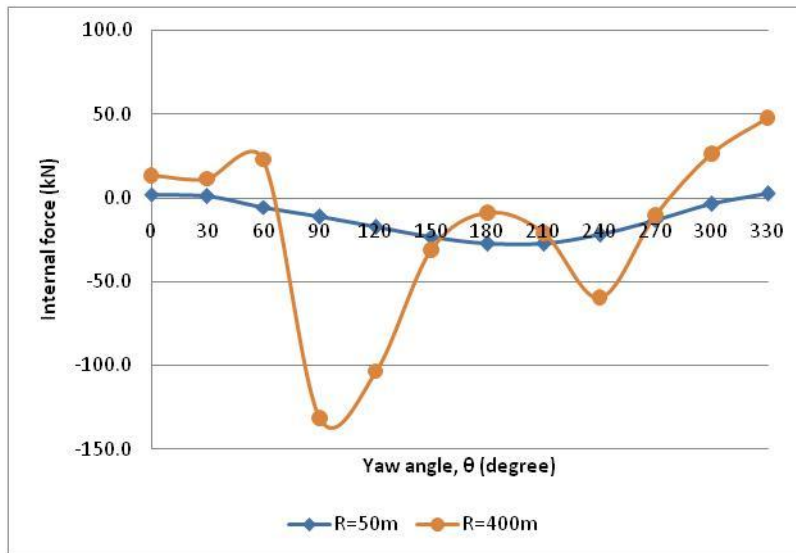


Fig. 9 Variation of the internal force in lower chord member #876 for various values of θ

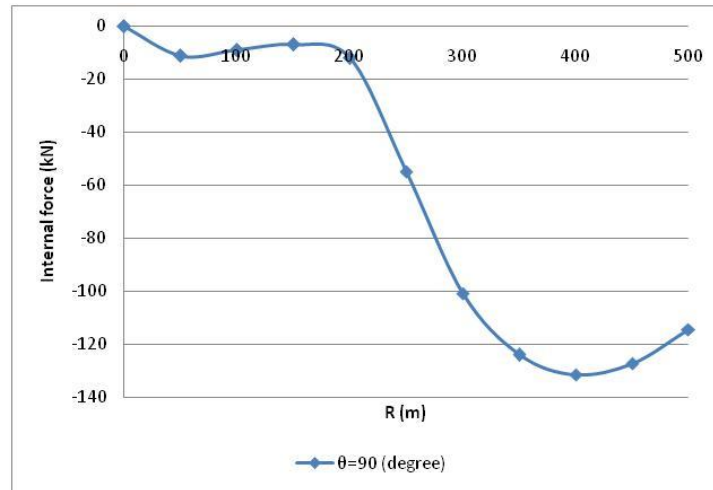


Fig. 10 Variation of the internal force in lower chord member #876 for various values of R

The following observations were drawn from the results shown in the figures above:

- The member internal forces were highly dependent on the tornado location, specified by the parameters R and θ .
- For a given R value, the tower's main chord members (#84) were subjected to high tensile as well as high compressive stresses while the cross-arms' chord members (#928, #876) were mainly subjected to high compressive stresses.
- With the exception of the upper chord member #928, for a constant θ value, the variation of R did not affect the type of internal force experienced by the members.
- For two constant R values, the variation of the members' internal forces was more pronounced for the larger R value.
- With the exception of the cross-arm chord members (#928, #876), the effect of varying the value of R on the members' internal forces was more pronounced for R values less than or equal to 200 m.
- With the exception of the cross-arm chord members (#928, #876), the members' internal forces followed a sine-wave curve due to varying values of θ .
- The effect of varying the value of R on the cross-arm chord members was more pronounced for R values between 200 m and 400 m.
- The effect of varying the value of θ on the cross-arm chord members was more pronounced for θ values between 60° and 150° .

8. Behaviour of transmission towers under tornado loads

This section attempts to explain the behaviour of the considered transmission line when subjected to tornado loading by interpreting the results of the analysis under the axi-symmetric F4 tornado wind field. A schematic diagram of the transmission tower is shown in Fig. 11. The tower acted as a cantilever beam subjected to a distributed load F due to the tornado wind on the tower, and three concentrated point loads due to the forces acting on the ground wires and conductors.

The results shown in Table 1 indicate that the critical tornado locations leading to the maximum axial forces for diagonal (1) members were located at distances R that ranged between 150 m to 400 m and between 270° to 330° for the angle θ . It is expected for diagonal (1) members, which were located on a plane perpendicular to the transmission line, to have a critical angle θ that placed the tornado on or close to the transmission line.

This configuration led to maximum external forces acting in the direction perpendicular to the line. This prediction matched the obtained results for 5 out of the 6 diagonal (1) members. The remaining diagonal (1) member had a critical angle θ of 330° . This was mainly due to two reasons. The first reason is that most diagonal members were located on planes that are not perfectly vertical, but are rather inclined toward the middle of the tower. This caused the external forces due to the critical tornadoes perpendicular to the transmission line to have a parallel force component that was applied to the diagonal (1) members. The second reason is that the diagonal members on the latticed plane were arranged in a wide range of configurations which caused some of the diagonal members to have a larger projected area value in the other direction.

The results shown in Table 1 indicate that the critical tornado locations leading to the maximum axial forces in diagonal (2) members were located at distances R that ranged between 150 m and 350 m and between 0° and 330° for the angle θ . Diagonal (2) members are expected to have a critical angle θ that places the tornado perpendicular to the transmission line. This configuration led to maximum external forces acting in the direction parallel to the line. This prediction matched the obtained results for only 3 out of the 6 diagonal (2) members. The remaining diagonal (2) members had critical angles θ of 120° and 270° . Most of the diagonal (2) members had critical tornado location that was different than the critical tornado locations associated with the surrounding diagonal members. The two reasons mentioned above were also the cause of this variation. For this reason, the behaviour of the diagonal members under tornado loading would be best described as random. This is acceptable since the axial forces in diagonal members due to F4 tornado loading were always less than the compression capacities of the members. Diagonal members are mainly used to provide adequate bracing for chord members in order to decrease the chords' unsupported lengths. They also provide redundancy and stiffness to the structure. This indicates that a different load case such as ice, failure containment, or maintenance typically governs the design of such members in transmission towers.

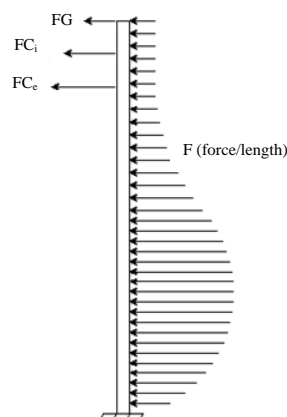


Fig. 11 Schematic diagram of the tower as a cantilever

As discussed earlier, a tornado configuration having R between 300m and 350m, and a $\theta=300^\circ$ was shown to lead to maximum compression forces in many chord members in zones 1 to 4. Also, a critical tornado location with $R=450$ m and $\theta=90^\circ$ was shown to be critical for the upper and lower chord members of the cross arm. Table 1 indicates that for zone 6, which was located above the cross-arms, the critical configuration leading to maximum compression was $R=250$ m and $\theta=270^\circ$. The following section focuses on describing the behaviour of the tower under the first and second critical configurations. The third configuration is not treated as an independent case, due to its proximity to the tornado location associated with case one.

8.1 Case 1: zones 1 to 5 ($R=300$ m to $R=350$ m and $\theta=300^\circ$)

Modelling the tower as a simple cantilever beam, as shown in Fig. 11, indicates that both the distributed load and the concentrated loads had the same effect on the straining action that developed in these zones. In other words, either a large distributed load along the beam or large concentrated loads at the top of the beam would lead to critical axial forces in the members in zones 1 to 5. Fig. 12 shows the location of the tornado relative to the tower of interest together with the deflected shape of the conductors adjacent to the tower. The deflections of the tower along the height in the X- and Y-directions are provided in Fig. 13. The deflected shapes show that a significant portion of the loading on the tower was in the transverse direction, along the X-axis.

The total horizontal velocity applied on the conductors was the vectorial sum of both tangential and radial velocity components. In this configuration, where the tornado was located at a radial distance R between 300 m and 350 m and $\theta=300^\circ$, a large section of the conductors in the two spans adjacent to the tower of interest was subjected to a uniform transverse loading, as can be seen in Fig. 12. The near symmetrical shape of the deflected conductors meant that the tower was subjected to large transverse loading (FG_{tran} , FC_{itrans} , and FC_{etran}), accompanied by minimal longitudinal forces (FG_{long} , FC_{ilong} , and FC_{elong}). This, in turn, subjected the tower to a uniaxial bending moment in the transverse direction. This large bending moment subjected two legs of the tower to tensile stresses while the other two legs were mainly subjected to compressive stresses.

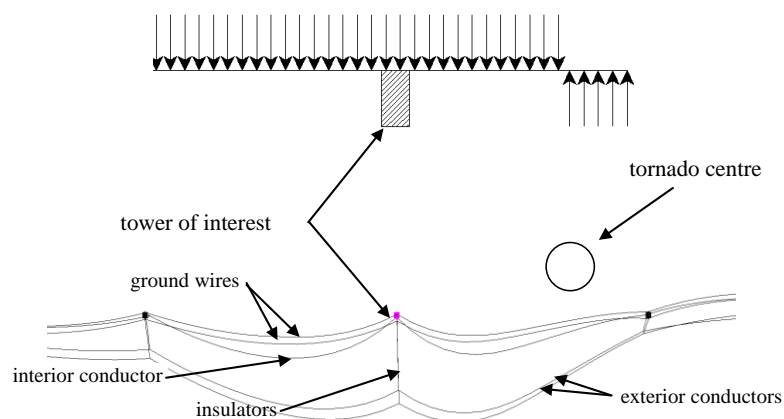


Fig. 12 Deflection shape and transverse loading of transmission line due to tornado centre at $R=300$ m and $\theta=300^\circ$

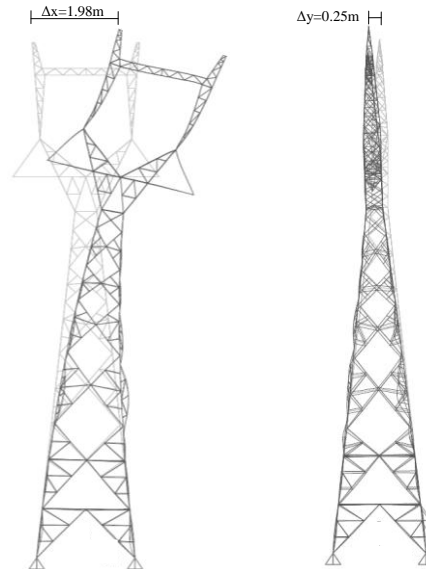


Fig. 13 Deflection shape of transmission tower due to tornado centre at $R=300$ m and $\theta = 300^\circ$

8.2 Case 2: cross-arms zone 5 ($R=400$ m to $R=450$ m and $\theta=90^\circ$)

The location of the tornado relative to the tower of interest corresponding to this critical case is shown in Fig. 17. Fig. 15 to Fig. 18 will assist in explaining why this tornado location is critical for the tower's cross-arms. In this configuration where the tornado was located along the transmission line, the conductors were subjected only to the tangential velocity component. A longitudinal axial force developed in the conductors due to catenary action associated with the transverse deflection of the conductors. As such, a variation in the magnitude of transverse deflection between the two spans adjacent to the tower led to resultant force acting on the insulators and on the tower's cross-arms (FC_{elong}), as shown in Fig. 14.

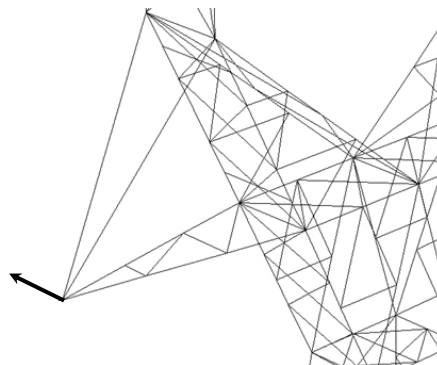


Fig. 14 Concentrated load in longitudinal direction due to left conductor associated with tornado at $R=400$ m and $\theta = 90^\circ$

This force caused an out-of-plane bending that acted on the cross-arms. This subjected one side of the cross-arm to compression and the other side to tension. Fig. 15 to Fig. 18 show that the conductors' deflections varied significantly with the relative distance R . The maximum deflection of the conductors occurred for R value between 400 m and 450 m. This value was approximately equal to 420 m, which was the horizontal span of the conductors. The angle θ having a value of 90° was critical because it allowed the full magnitude of the tangential velocity component to be applied in the transverse direction on the cables. This led to a large compressive force to develop in the cross-arms upper chord members. The upper chord member, #928 had a large unsupported length. This indicated that it might have been designed to resist tension forces, which were mainly due to the conductors' own weight.

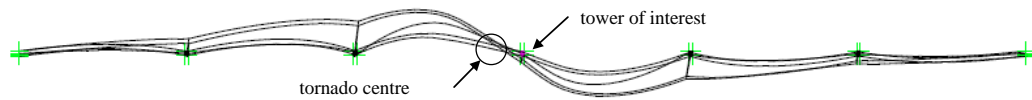


Fig. 15 Deflection shape of transmission tower due to tornado centre at $R=50$ m and $\theta = 90^\circ$

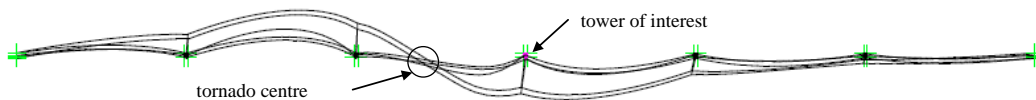


Fig. 16 Deflection shape of transmission tower due to tornado centre at $R=250$ m and $\theta = 90^\circ$

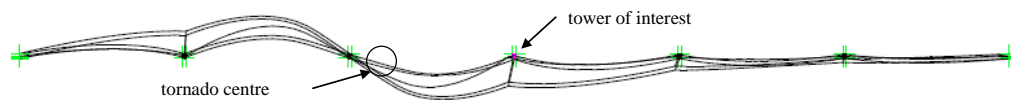


Fig. 17 Deflection shape of transmission tower due to tornado centre at $R=400$ m and $\theta = 90^\circ$

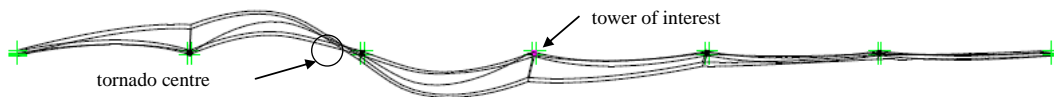


Fig. 18 Deflection shape of transmission tower due to tornado centre at $R=450$ m and $\theta = 90^\circ$

9. Conclusions

The following conclusions were drawn from the conducted study:

- The location of the tornado with respect to the tower of interest, which was defined in terms of the polar parameters R and θ , had a significant effect on the forces in the tower members.

- Different member types had independent critical values of R and θ that led to peak forces. Therefore, it is important to conduct an extensive parametric study similar to the one conducted in the study in order to determine the peak forces in all members of the tower.
- A member's type and location influenced the location of the tornado associated with the peak force for such a member.
- The F4 tornado responsible for the peak forces in the main body's chord members was located at a value R of 300 m and a value θ of 300° .
- The F4 tornado responsible for the peak forces in the cross-arms chord members was located at a value θ of 90° and at a distance R approximately equal to the horizontal span of two consecutive transmission towers.
- The difference between the axial forces resulting from the axi-symmetric F4 and the three-dimensional F4 data was relatively small. The difference between the axial forces resulting from both analyses was more significant in the lower part of the tower. This variation was mainly due to the significant wind instability in the lower region of the tornado system, which could only be modelled in the three-dimensional analysis.
- The majority of the critical tornado locations were the same under both the axi-symmetric F4 tornado wind field and the three-dimensional F4 tornado wind field.
- For most of the selected members, the value of the parameter θ describing the critical F2 tornado location was the same as that describing the location of the critical F4 tornado. However, this was not the case with the value of the parameter R due to the variation of the vertical velocity profiles between the F2 and F4 tornadoes.
- For a given member, the critical tornado location associated with the peak tensile load had the same R value as the critical tornado location associated with the peak compressive load. For the same member, the values of θ associated with the peak tensile and compressive loads were 180° apart.
- The axial forces due to normal wind were comparable to those due to F2 tornado. This suggests that it should be economically feasible to design and retrofit existing transmission lines such that they are able to resist to forces of an F2 tornado.
- The simplified F2 tornado loading recommended by CIGRE produced axial compressive loads that were smaller than the loads due to the three-dimensional F2 tornado wind field in members located in the main body of the tower, in zones 1 to 3, and 6. The axial forces in zones 4 and 5 due to the CIGRE loading were significantly higher than those due to F2 tornado loading. The discrepancy in the axial forces in zones 4 and 5 was due to the failure containment loading condition suggested by CIGRE.
- CIGRE simplified tornado loading underestimated the axial tensile forces in zones 1 to 3, and 6 when compared to the tensile forces resulting from the three-dimensional F2 tornado wind field. However, it overestimated the tensile forces in chord members located in zones 4 and 5. This was caused by the failure containment load case suggested by CIGRE.
- The upper chord member of the cross arm was subjected to large compressive axial force under CIGRE-simplified tornado loading. This could also be attributed to the failure containment load case, which subjected the transmission tower to unbalanced loading condition. This unbalanced loading, on the other hand, was inherently included in the 3-D tornado wind field used.
- The sensitivity analysis indicated that for two constant R distances, the members' axial forces associated with the larger R value experienced a larger variation.

References

- Ahmad, S. and Ansari, E. (2009), "Response of transmission towers subjected to tornado loads", *Proceedings of the 7th Asia-Pacific Conference on Wind Engineering*, Taipei, Taiwan, November.
- American Meteorological Society (2000), *Glossary of Meteorology*, AMS, Boston, Massachusetts, U.S.A.
- American Society of Civil Engineers (ASCE) (2000), *ASCE Standard 10-97*, Design of Latticed Steel Transmission Structures, New York, U.S.A.
- American Society of Civil Engineers (ASCE) (1991), *ASCE Manuals and Reports on Engineering Practice No. 74*, Guidelines for electrical transmission line structural loading, Reston, Virginia, U.S.A.
- American Society of Civil Engineers (ASCE) (2005), *ASCE Manuals and Reports on Engineering Practice No. 74 draft revision*, Guidelines for electrical transmission line structural loading, Reston, Virginia, U.S.A.
- American Society of Civil Engineers (ASCE) (2010), *ASCE Manuals and Reports on Engineering Practice No. 74*, Guidelines for electrical transmission line structural loading third edition, Reston, Virginia, U.S.A.
- Behncke, R., White, H. and Milford, R. (1994), "High intensity wind and relative reliability based loads for transmission line design", *Proceedings of the International Conference on Large High Voltage Electric Systems*, Paris, France.
- Canadian Standards Association (CSA) (1976), *CAN/CSA-C22.3 No.1*, Overhead Systems, Montreal.
- CIGRE, (International Council on Large Electric Systems) (2009), *Overhead line design guidelines for mitigation of severe wind storm damage (SC B2.39)*, Committee Draft, Paris, France.
- Computer and Structures Inc. (2008), *CSI:SAP2000 Analysis Reference Manual*, Computer and Structures Inc., Berkeley, California, USA.
- Darwish, M.M., El Damatty, A.A. and Hangan, H. (2010), "Dynamic characteristics of transmission line conductors and behaviour under turbulent downburst loading", *Wind Struct.*, **13**(4), 327-347.
- Dempsey, D. and White H. (1996), "Winds wreak havoc on lines", *Transmission Distribution World*, **48**(6), 32-37.
- Fluent Inc. (2005), *Fluent 6.2 User's Guide*, Fluent Inc., Lebanon.
- Fujita, T. (1981), "Tornadoes and downbursts in the context of generalized planetary scales", *J. Atmos. Sci.*, **38**(8), 1511-1534.
- Hamada, A., El Damatty, A.A., Hangan, H. and Shehata, A.Y. (2010), "Finite element modelling of transmission line structures under tornado wind loading", *Wind Struct.*, **13**(5), 451-469.
- Hamada, A. and El Damatty, A.A. (2011), "Behaviour of guyed transmission line structures under tornado wind loading", *Comput. Struct.*, **89**(11-12), 986-1003.
- Hangan, H. and Kim, J. (2008), "Swirl ratio effects on tornado vortices in relation to the Fujita scale", *Wind Struct.*, **11**(4), 291-302.
- Ishac, M. and White, H. (1995), "Effect of tornado loads on transmission lines", *IEEE T. Power Deliver.*, **10**, 445-451.
- Lahey Computer Systems Inc. (1999), *LF Fortran Express User's Guide*, Lahey Computer Systems, Inc., Incline Village, Nevada, USA.
- Langlois, S. (2007), *Design of overhead transmission lines subject to localized high intensity wind*, Master of Engineering Thesis, McGill University, Montreal.
- Lee, W.C. and Wurman, J. (2005), "Diagnosed three-dimensional axisymmetric structure of the Mulhall tornado on 3 May 1999", *J. Atmos. Sci.*, **62**, 2373-2393.
- Matheson, M.J. and Holmes, J.D. (1981), "Simulation of the dynamic response of transmission lines in strong winds", *Eng. Struct.*, **3**(2), 105-110.
- McCarthy, P. and Melsness, M. (1996), *Severe weather elements associated with September 5, 1996 hydro tower failures near Grosse Isle, Manitoba, Canada*, Manitoba Environmental Service Centre, Environment Canada.
- National Research Council of Canada (NRCC) (1990), *Supplement to the National Building Code of Canada*, Ottawa.

- Sarkar, P., Haan, F., Gallus, W. Jr., Kuai, Le. and Wurman, J., (2005), "Velocity measurements in a laboratory tornado simulator and their comparison with numerical and full-scale data", *Proceedings of the 37th Joint Meeting Panel on Wind and Seismic Effects (UJNR)*, Tsukuba, Japan, May.
- Savory, E., Parke, G.A., Zeinoddini, M., Toy, N. and Disney, P. (2001), "Modelling of tornado and microburst-induced wind loading and failure of a lattice transmission tower", *Eng. Struct.*, **23**(4), 365-375.
- Shehata, A.Y., El Damatty, A.A. and Savory, E. (2005), "Finite element modelling of transmission line under downburst wind loading", *Finite Elem. Anal. Des.*, **42**(1), 71-89.
- Wen, Y.K. (1975), "Dynamic tornadic wind loads on tall buildings", *J. Struct. Eng. - ASCE*, **101**(1), 169-185.

JH